OPEN

Correspondence and
requests for materials
should be addressed to
Y.L. (liuyu@xzmc.edu.
cn)

Motor preparation attenuates neural variability and beta-band LFP in parietal cortex

Mo Chen[1,2], Linyu Wei[3] & Yu Liu[1,2]

[1]Jiangsu Province Key Laboratory of Anesthesiology and Jiangsu Province Key Laboratory of Anesthesia and Analgesia Application Technology, Xuzhou Medical College, Xuzhou, China, 221004, [2]Institute of Neuroscience, Shanghai Institutes for Biological Sciences, Chinese Academy of Sciences, and University of Chinese Academy of Sciences, Shanghai, China, 200031, [3]Department of Physiology and Neurobiology, Xinxiang Medical University, Xinxiang, China, 453003.

Accumulative evidence shows that neural variability is meaningful and powerful during brain information processing, but how cognitive state influences neural variability is still unclear. We studied neural variability during motor preparation in lateral intraparietal area (LIP), a brain area closely involved in saccade generation. During motor preparation, we observed significant variability decline, and the decline highly correlated with beta-band local field potential (LFP) fluctuations. Furthermore, we found similar variance-LFP correlations in both the memory-guided saccade task and the visually-guided saccade task. These results indicate a possible linkage between beta-band LFP and trial-to-trial neural variability.

In 1926, when E. D. Adrian and Y. Zotterman evaluated the response levels of sensory nerve fibres to stimulations on their end-organs, they counted the total number of impulses in each second[1]. Following this pioneering work, numerous researchers employ the so-called rate coding, and make great achievements. By computing the mean firing rate, the rate coding evaluates the firing state on expense of ignoring neural variability. However, more and more evidence suggests that neural variability is not simple 'neural noise', but should be meaningful to the central nervous system[2,3]. Also, it is plausible to assume that part of the variability is caused by some hidden factors which the researchers just do not realize[4].

A representative statistical measure of neural variability is the ratio of spike count variance to spike count mean (the Fano factor). Fano factor is quenched by the stimulus onset across many brain areas, including V1, V4, MT, LIP, etc[5]. Besides the external stimulation, an increasing number of studies have found that internal brain states, such as attention[6,7] and motor preparation[8–10], also modulate neural variability. But there are also controversial results indicating that the neural variability of frontal eye field (FEF) neurons is not modulated by attention[11].

To study the mechanism of neural variability, we resorted to another neural signature, the local field potential (LFP), which mainly reflects local synaptic potentials[12,13]. There is plenty of evidence suggesting linkages between LFP and cognitive processes, such as intention[14], attention[15], perception[16] and memory[17].

We employed a classical motor preparation task, the gap task, to investigate the effect of the internal brain state on neural variability in lateral intraparietal area (LIP). LIP is a brain area strongly involved in saccade execution. By using the extracellular recording technique, we recorded the LFP and the single-unit activity in LIP simultaneously. In the gap task, the Fano factor significantly declined during the gap period, which might be caused by the general motor preparation. Furthermore, the low-frequency LFP power, especially in the beta-band, decreased during the gap period. And there existed a fine correlation between Fano factor and low-frequency LFP power. We also observed such correlations in the memory-guided saccade task and the visually-guided saccade task. These results offer us a hint about the linkage between neural variability and LFP.

Results and Discussion

To investigate the influence of cognitive processes on neural variability, we trained two monkeys (*Macaca mulatta*) to perform the gap task. In the gap task, each trial began with a fixation point appearing on the center of the screen (Fig. 1a). After the fixation point offset, the gap period started during which there was no visible stimulus on the screen. At the end of the gap period, a peripheral saccade target appeared which would randomly appear in the recorded neuron's receptive field (RF) or in the opposite direction (OPPO-RF). In consistence with previous findings[18,19], the gap period not only dramatically shortened the saccade latency, but also led to the
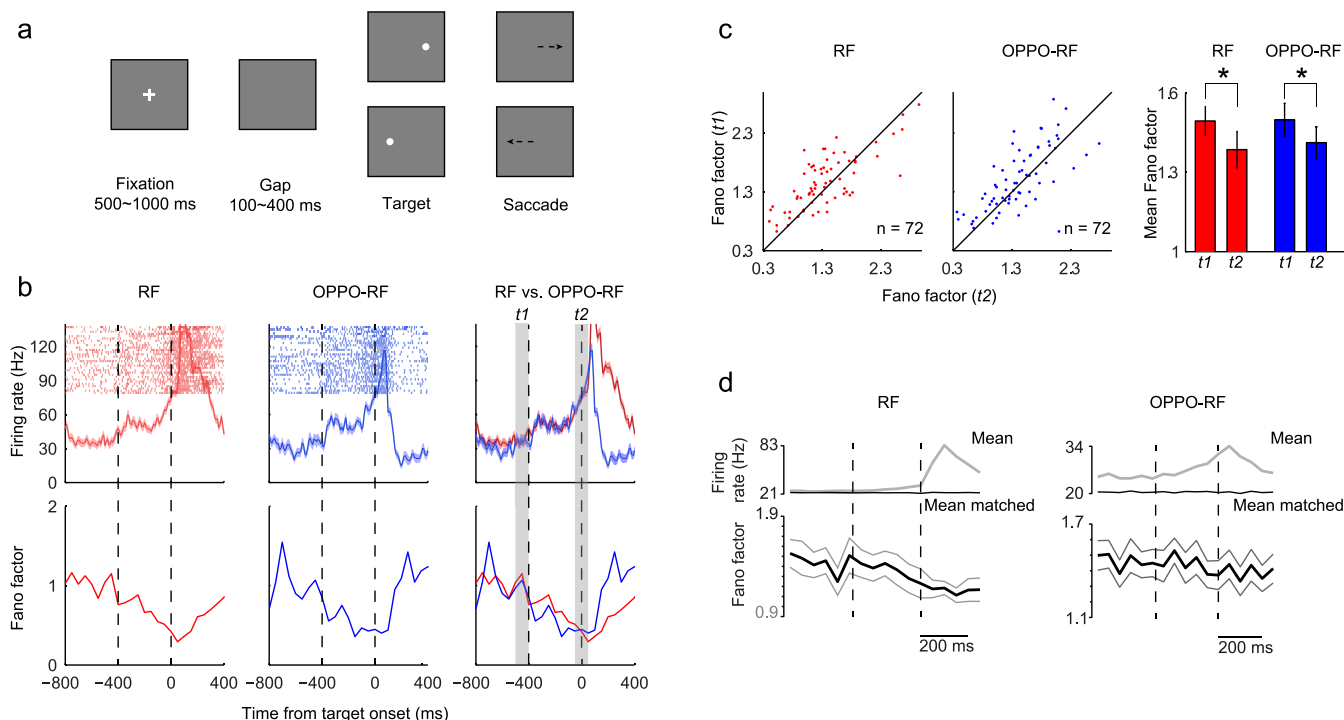
Figure 1 | Paradigm, LIP neural activity and neural variability. (a), Gap task. Each trial began with the appearance of a central fixation point. Between the fixation point offset and the saccade target onset, there was a blank gap period during which animals were required to continue fixating the center of the screen. After the target onset, animals were rewarded for making a saccade to the target. (b), The firing rate (first row) and Fano factor (second row) of an example neuron in the gap task. Data of the RF (first column) and OPPO-RF (second column) conditions are superimposed in the third column. *t1*: baseline period, 0–100 ms before the gap period, *t2*: the end of gap, from 50 ms before to 50 ms after the saccade target onset. (c), Comparisons of Fano factor between *t1* and *t2* for all neurons. The Fano factor was significantly lower in *t2* than that in *t1* (RF, $p = 0.016$; OPPO-RF, $p = 0.044$, *t*-test). (d), The mean firing rate (gray), mean-matched firing rate (black) and Fano factor (black with flanking s.e.m.) of all neurons in the gap task. The Fano factor was computed after mean-matching. Two vertical dashed lines indicate the gap period.

bimodally-distributed saccade latency (Supplementary Fig. S1). The neuronal activity of LIP gradually increased during the gap period (Supplementary Fig. S2), which we have partially reported previously[20].

Across-trial neural variability during motor preparation. During this 'motor preparation' period, the trial-to-trial variability (measured by Fano factor) greatly declined. As shown in Figure 1b, the neural variability of an example neuron gradually declined in the gap period, regardless whether the target appeared in the neuron's receptive field (RF, red line) or in the opposite direction (OPPO-RF, blue line). Compared with baseline (*t1*, the final 100 ms before the fixation point offset), the Fano factor of this example neuron at the end of gap (*t2*, from 50 ms before to 50 ms after the saccade target onset) declined 58.5% in the RF condition and 55.9% in the OPPO-RF condition, respectively.

The Fano factor distributions of 72 neurons (monkey S, 49; monkey P, 23) during *t1* and *t2* intervals were shown in Figure 1c. In the RF condition, 68% neurons exhibited lower Fano factor in *t2* compared with that in *t1*, and the ratio was 63.9% in the OPPO-RF condition. Statistically, the Fano factor in *t2* was significantly lower than that in *t1* in both RF ($p = 0.016$, paired *t*-test) and OPPO-RF ($p = 0.044$, paired *t*-test) conditions.

To rule out the possibility that the variability decline is merely caused by rising firing rate, we employed a mean-matching method to calculate the Fano factor (see Methods)[5]. During the gap period, the mean-matched Fano factor clearly declined across the population (Fig. 1d). And the raw data of spike count variance versus spike count mean also showed similar results (see Supplementary Fig. S3).

LFP fluctuations during motor preparation. Besides the variability decline, the low-frequency LFP fluctuations were also suppressed

during motor preparation. To analyze the LFP power spectrum, the visual-evoked potential was discarded (see Methods). Figure 2a shows the LFP traces of two example trials: one is the RF trial, and the other is the OPPO-RF trial. The amplitudes of LFP fluctuations clearly declined at the end of gap compared with that in the fixation period. We analyzed the LFP power of these two trials in different frequency bands (Fig. 2b). For frequencies less than 40 Hz, the LFP power during *t2* was all lower than that during *t1* (the largest *p* value is 0.035, *t*-test), and the largest LFP power difference appeared around 15.6 Hz in both the RF and OPPO-RF conditions.

During motor preparation, the LFP power across the population in the low-frequency band also decreased (Fig. 2c). From *t1* to *t2*, the time-frequency spectra showed local power decreases between 10 and 37 Hz in the RF condition and between 10 and 41 Hz in the OPPO-RF condition ($p < 0.05$, *t*-test), both of which mostly fell into the beta-band (13–30 Hz). The largest power decrease occurred around 27 Hz in the RF condition (1.46% decrease) and 28 Hz in the OPPO-RF condition (1.47% decrease), respectively.

The correlation between neural variability and LFP in the gap task. Based on the observed decreases of trial-to-trial variability and low-frequency LFP power during motor preparation, we further examined whether they were correlated. The correlation coefficient between the Fano factor of each neuron and the 23.44 Hz LFP power recorded simultaneously in *t2* was calculated (Fig. 3a). Here we specifically picked 23.44 Hz based on the results from Figure 2c. The correlation coefficients in the RF and OPPO-RF conditions were 0.4483 ($p < 0.001$, *F*-test) and 0.4187 ($p < 0.001$, *F*-test), respectively.

For the broader frequency band of LFP, the correlations between Fano factor and LFP power exhibited fine frequency-dependent rela-
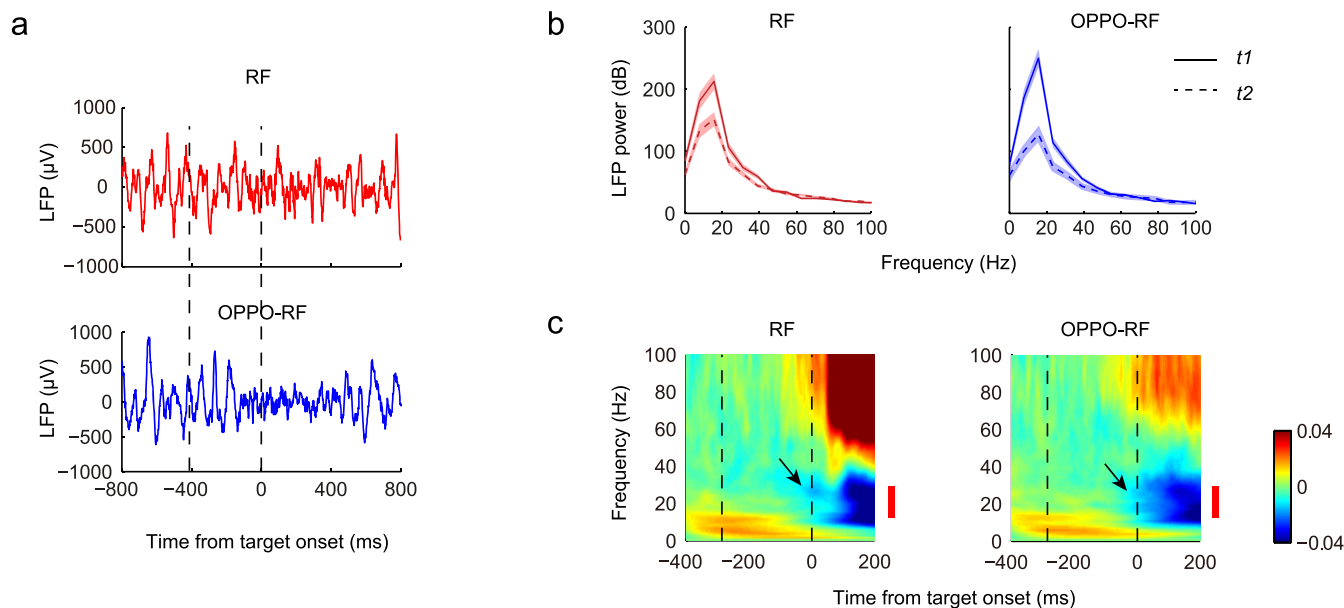
Figure 2 | LFP fluctuations in the gap task. (a), Examples of the single-trial LFP trace. The visual-evoked potential was discarded (see Methods). Data are from the same example neuron in Figure 1b. Two vertical dashed lines indicate the gap period. (b), Comparisons of LFP power between *t1* (solid line) and *t2* (dashed line) among all trials of the same example neuron. Flanking traces give s.e.m. (c), Time-frequency maps of spectral power, normalized to baseline. Data are from all recorded LIP neurons and are aligned on the target onset. Two vertical dashed lines indicate the averaged gap interval of all recorded neurons. Red bars denote the beta-band LFP (13–30 Hz). Black arrows denote the major LFP power decreases in *t2*, which mainly occurred in the beta-band.

tionship (Fig. 3b). Since there were scattered significant data points, to clearly present the data, here only consecutive significant points containing no less than 5 significant data points were considered to be significant ($p < 0.05$, F-test), and are indicated by thicken lines. In the RF and OPPO-RF conditions, the significant frequency bands were 0–35.16 Hz and 7.81–46.88 Hz, respectively. These significant LFP bands also mostly fell into the beta-band.

Based on these results, we made special effort to investigate the low-frequency LFP (< 60 Hz) in the following analysis. The time-frequency maps of correlation coefficients revealed that the Fano factor and beta-band LFP power were mostly positively correlated during the gap period (Fig. 3c). At the end of the gap period, there was significant correlation between 23 and 31 Hz in the RF condition ($p < 0.05$, F-test), and the significant correlation band was 23–43 Hz in the OPPO-RF condition ($p < 0.05$, F-test).

The correlations between neural variability and LFP in other tasks. Besides the gap task, we also studied the Fano factor changes and the LFP fluctuations in the visually-guided saccade task (Supplementary Figs. S4 and S5) and in the memory-guided saccade task (Supplementary Figs. S6 and S7). In the visually-guided saccade task, the mean-matched Fano factor clearly declined immediately after the target onset (Supplementary Fig. S4), which is consistent with previous study[5]. Compared with the baseline period (300–400 ms before the target onset), the LFP power spectrum showed local decreases in the low-frequency band after the target onset (150–250 ms after the target onset; Supplementary Fig. S5a), especially between 8 and 30 Hz ($p < 0.05$, paired t-test). Furthermore, there was significant positive correlation between Fano factor and LFP power after the target onset, which was between 19.5 and 39.0 Hz ($p < 0.05$, paired t-test; Supplementary Fig. S5b).

In the memory-guided saccade task, in consistence with previous findings in dorsal premotor cortex (PMd)[8], the Fano factor declined after the target onset, and then rose up, but remained at a lower and rough plateau during the delay period (Supplementary Fig. S6). The spectrogram of LFP was similar to previous study in LIP[17], which

showed elevated power in the gamma-band (30–100 Hz) after the target onset and sustained elevation during the memory period (especially around 50–70 Hz; Supplementary Fig. S7a). The correlation between Fano factor and LFP was high mainly in two periods (Supplementary Fig. S7b): the first high correlation peak appeared around 500 ms after the target onset; the other peak appeared around the fixation point offset. Consistent with our findings in the gap task and in the visually-guided saccade task, the high correlation around the fixation point offset mainly occurred in the beta-band (23.4–43.0 Hz; $p < 0.05$, F-test).

Our recording results from LIP showed that the neural variability declined during motor preparation. Together with previous studies, we conclude that motor preparation would reduce neural variability in at least several brain areas, including PMd, V4 and LIP. By reducing the neural variability, motor preparation not only 'prepares' these areas, but also stabilizes them.

More interestingly, there existed fine correlations between low-frequency LFP power and single-unit neural variability in all three tasks, especially in the beta-band: the neural variability is more likely to be low if the beta-band LFP power is attenuated, and vice versa.

Although the present study cannot tell the causality between neural variability and LFP fluctuations, which requires strictly designed paradigms and vast studies in other brain areas, based on our experimental data and understandings we tend to believe that motor preparation would cause both neural variability decline and beta-band LFP power decrease in related brain areas, and these two neural mechanisms should act in a complementary way.

Methods

Subjects. Two male monkeys (*Macaca mulatta*, 5–7 kg) were the subjects of the present study. General surgical procedures have been reported previously[20].
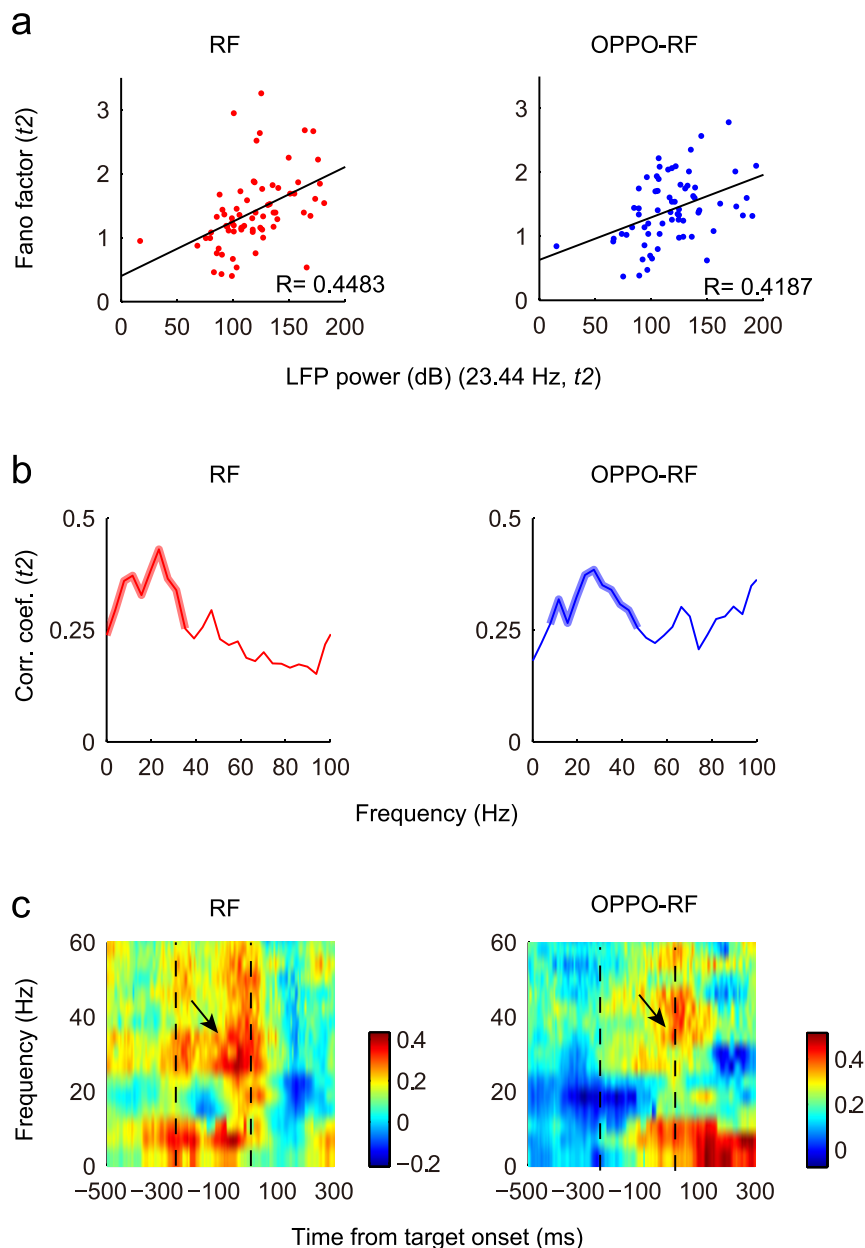
Figure 3 | Correlation between neural variability and LFP power. (a), The correlation between neural variability and 23.44 Hz LFP power in *t2*. Each dot represents the Fano factor of one neuron and the LFP recorded simultaneously. Black lines represent the linear regression. The correlation coefficients in the RF and OPPO-RF conditions were 0.4483 ($p < 0.001$, *F*-test) and 0.4187 ($p < 0.001$, *F*-test), respectively. (b), The distributions of correlation coefficients in *t2* period in different frequency bands. Thicken lines indicate the significant correlation ($p < 0.05$, *F*-test). (c), Two-dimensional plots of the correlation coefficients. Time is on the *x*-axis; Frequency is on the *y*-axis. Correlation coefficient is color-coded on a linear scale. Two dashed lines indicate the averaged gap period. Black arrows denote the high correlation coefficients in *t2*.

Experimental procedures. Experiments were carried out in a dark environment. During experiments, monkeys were seated inside a primate chair with their heads firmly fixed to the chair. A 21-inch CRT monitor was placed 55 cm in front of the monkeys. Visual displays were under the control of a QNX computer running a real-time data acquisition system (REX; NIH, Bethesda, MD). The storages of both neuronal activity and eye position data were under Cerebus (Blackrock Microsystems). Eye movements were recorded with the magnetic search coil technique[21], which had a resolution of 0.1°. Horizontal and vertical eye position data were collected at 1 kHz frequency. Tungsten microelectrodes (~1 MΩ at 1 kHz) were lowered through 23 gauge stainless steel guide tubes by an electronic microdrive (NAN Instruments) attached to the recording chambers, and the extracellular neuronal activity was recorded.

Behavioral paradigms. Three behavioral tasks were employed in present study, i.e., the gap task, the memory-guided saccade task and the visually-guided saccade task.

Gap task. Each trial began with the appearance of a white cross (fixation point) on the center of the screen (Fig. 1a). The fixation point duration was 500–1000 ms. After

the fixation point offset, the gap period started during which there was no visible stimulus on the screen, and monkeys were trained to maintain fixation on the center of the screen. Within a session, the gap duration was constant. The gap interval was 200–400 ms for monkey S, and was 100–200 ms for monkey P. In each session, the optimal gap duration was chosen based on the animal behavior performance, in order to produce a bimodal distribution profile of saccadic latency[22,23]. At the end of the gap period, the saccade target appeared either in the recorded neuron's receptive field (RF) or in the equidistant location in the opposite hemisphere (OPPO-RF). Monkeys should make a saccade to the target (within 500 ms) and then maintained fixation for 400 ms before receiving a drop of juice as the reward.

Memory-guided saccade task. The memory-guided saccade task was used to find LIP and to classify recorded neurons. Each trial began with the appearance of a white cross, the fixation point, on the center of the screen. Monkeys were trained to fixate the fixation point as long as it was on the screen. After monkeys fixating the fixation point for 500 ms, a visual target appeared briefly (200 ms) at one of eight possible locations. The eight possible locations distributed evenly around the fixation point and positioned at an equal eccentricity (12°). The duration of the fixation point was

1700–2000 ms. Monkeys had to maintain fixation until the fixation point offset, after which they made a single saccade toward the remembered target location. Successful trials were rewarded.

Visually-guided saccade task. Each trial began when a white cross (fixation point) appeared on the center of the screen, and monkeys were trained to fixate it. When the fixation point disappeared, a peripheral visual target appeared simultaneously. The target always appeared in the recorded neuron's receptive field. Monkeys were rewarded for making a saccade to the target.

Behavioral data analysis. Criteria for saccades. The start and end of a saccade were determined by the velocity threshold and the template matching criteria[24]. The initiation of a saccade was identified when the velocity of eye movement exceeded $20°/s$ and this high velocity lasted for more than 10 ms. Saccades satisfying the following criteria were analyzed: (1) saccade occurred after the visual target onset; (2) saccade duration was 10–200 ms; and (3) saccadic endpoint fell into the 5° window which centered at the saccadic target.

Criteria for express and regular saccades. To prevent arbitrary separation of express saccades and regular saccades in the gap task, a maximum likelihood estimation was applied to saccade latency distributions, to obtain the best fit of the two modes for each monkey[25] (Supplementary Fig. S1). The intersection point of the two modes of generalized extreme value (GEV) fitting was defined as the boundary between express saccades and regular saccades. For monkey S the boundary was around 100 ms, and for monkey P the boundary was relatively longer, around 124 ms. Saccades with latency shorter than the boundary were defined as express saccades; otherwise, they were considered as regular saccades. Trials with latency less than 50 ms were considered as expected saccade trials and were excluded in present study.

Neuronal data analysis. Localizing LIP. LIP was localized by its signature in the memory-guided saccade task, i.e., the persistent activity during the memory period[26,27].

Spike density function. The firing rate was presented as spike density function, and the spike density function was aligned on specific event in each task. To generate the spike density function, a Gaussian pulse of specified width (10 ms) was substituted for each spike, and then all Gaussian pulses were summed to produce a continuous function of spike density.

Fano factor. Fano factor was calculated as the ratio of the spike count variance to the mean in a 50 ms window sliding in 10 ms steps. Windows containing no spike across trials were excluded from calculation. Fano factor was calculated separately in the RF and OPPO-RF conditions.

Mean-matching method. The mean-matching method was first demonstrated by Churchland and colleagues[5], so please refer to the original paper for detailed information. Generally, this method was aimed at minimizing the possibility that the declining Fano factor was merely caused by rising firing rate. First, for all recorded neurons, the distributions of mean spike counts for each time point and condition were calculated. Then we calculated the greatest common distribution, and selected neurons matching this distribution at each time point and condition. The Fano factor was then computed. So at each time point, a different group of neurons were used.

Local field potential analysis. LFP data were filtered between 0 and 300 Hz and digitized at 1 kHz. To remove the power line noise, the LFP data were filtered out using a 50 Hz notch filter. Slow fluctuations in electrophysiological signals and line noise were removed from LFP by using a local linear regression to detrend neural signals (Chronux 2.00 toolbox, http://www.chronux.org)[28]. Before applying further analyses, we first discarded the visual-evoked potential by subtracting the mean LFP of all trials from each single trial. Then the power spectrum of LFP was constructed for each trial by performing the fast-Fourier transform algorithm (FFT) using MATLAB version 7.9.0 and averaged across all trials for each condition.

Wavelet analysis. The wavelet transform was applied to analyze the time-dependent spectrum of LFP data. We convolved the LFP data with Morlet wavelet (f_0 = 0.849) by using a MATLAB wavelet software package provided by C. Torrence and G. Compo[29], which is available at URL: http://atoc.colorado.edu/research/wavelets/. The wavelet transform was applied to each individual LFP and the LFP power of each frequency band was normalized by the corresponding mean and standard deviation (SD) of that band.

Correlation between Fano factor and LFP power. The correlation coefficients between Fano factor and LFP power were computed using Pearson's correlation coefficient method. Data points with a difference >3 SDs from the mean were considered as outliers, and were excluded while calculating correlation coefficients. The correlation coefficients were calculated in a 200 ms window sliding in 5 ms steps.

1. Adrian, E. D. & Zotterman, Y. The impulses produced by sensory nerve-endings Part II. The response of a Single End-Organ. *J. Neurophysiol.* **61**, 151–171 (1926).
2. Stein, R. B., Gossen, E. R. & Jones, K. E. Neuronal variability: noise or part of the signal? *Nat. Rev. Neurosci.* **6**, 389–397 (2005).
3. Wiesenfeld, K. & Moss, F. Stochastic resonance and the benefits of noise: from ice ages to crayfish and SQUIDs. *Nature* **373**, 33–36 (1995).
4. Amarasingham, A., Chen, T.-L., Geman, S., Harrison, M. T. & Sheinberg, D. L. Spike count reliability and the Poisson hypothesis. *J. Neurosci.* **26**, 801–809 (2006).
5. Churchland, M. M. *et al.* Stimulus onset quenches neural variability: a widespread cortical phenomenon. *Nat. Neurosci.* **13**, 369–378 (2010).
6. Cohen, M. & Maunsell, J. Attention improves performance primarily by reducing interneuronal correlations. *Nat. Neurosci.* **12**, 1594–1600 (2009).
7. Mitchell, J. F., Sundberg, K. A. & Reynolds, J. H. Differential attention-dependent response modulation across cell classes in macaque visual area V4. *Neuron* **55**, 131–141 (2007).
8. Churchland, M. M., Byron, M. Y., Ryu, S. I., Santhanam, G. & Shenoy, K. V. Neural variability in premotor cortex provides a signature of motor preparation. *J. Neurosci.* **26**, 3697–3712 (2006).
9. Steinmetz, N. A. & Moore, T. Changes in the response rate and response variability of area V4 neurons during the preparation of saccadic eye movements. *J. Neurophysiol.* **103**, 1171–1178 (2010).
10. Falkner, A. L., Goldberg, M. E. & Krishna, B. S. Spatial Representation and Cognitive Modulation of Response Variability in the Lateral Intraparietal Area Priority Map. *J. Neurosci.* **33**, 16117–16130 (2013).
11. Chang, M. H., Armstrong, K. M. & Moore, T. Dissociation of response variability from firing rate effects in frontal eye field neurons during visual stimulation, working memory, and attention. *J. Neurosci.* **32**, 2204–2216 (2012).
12. Katzner, S. *et al.* Local origin of field potentials in visual cortex. *Neuron* **61**, 35–41 (2009).
13. Lindén, H. *et al.* Modeling the spatial reach of the LFP. *Neuron* **72**, 859–872 (2011).
14. Scherberger, H., Jarvis, M. R. & Andersen, R. A. Cortical local field potential encodes movement intentions in the posterior parietal cortex. *Neuron* **46**, 347–354 (2005).
15. Womelsdorf, T. & Fries, P. The role of neuronal synchronization in selective attention. *Curr. Opin. Neurobiol.* **17**, 154–160 (2007).
16. Gail, A., Brinksmeyer, H. J. & Eckhorn, R. Perception-related modulations of local field potential power and coherence in primary visual cortex of awake monkey during binocular rivalry. *Cereb. Cortex* **14**, 300–313 (2004).
17. Pesaran, B., Pezaris, J. S., Sahani, M., Mitra, P. P. & Andersen, R. A. Temporal structure in neuronal activity during working memory in macaque parietal cortex. *Nat. Neurosci.* **5**, 805–811 (2002).
18. Fischer, B. & Boch, R. Saccadic eye movements after extremely short reaction times in the monkey. *Brain Res.* **260**, 21–26 (1983).
19. Fischer, B. & Ramsperger, E. Human express saccades: extremely short reaction times of goal directed eye movements. *Exp. Brain Res.* **57**, 191–195 (1984).
20. Chen, M., Liu, Y., Wei, L. & Zhang, M. Parietal Cortical Neuronal Activity Is Selective for Express Saccades. *J. Neurosci.* **33**, 814–823 (2013).
21. Fuchs, A. & Robinson, D. A method for measuring horizontal and vertical eye movement chronically in the monkey. *J. Appl. Physiol* **21**, 1068–1070 (1966).
22. Dorris, M., Pare, M. & Munoz, D. Neuronal activity in monkey superior colliculus related to the initiation of saccadic eye movements. *J. Neurosci.* **17**, 8566 (1997).
23. Schiller, P. H., Haushofer, J. & Kendall, G. An examination of the variables that affect express saccade generation. *Vis. Neurosci.* **21**, 119–127 (2004).
24. Waitzman, D. M., Ma, T. P., Optican, L. M. & Wurtz, R. H. Superior colliculus neurons mediate the dynamic characteristics of saccades. *J. Neurophysiol.* **66**, 1716–1737 (1991).
25. Guan, S., Liu, Y., Xia, R. & Zhang, M. Covert attention regulates saccadic reaction time by routing between different visual-oculomotor pathways. *J. Neurophysiol.* **107**, 1748–1755 (2012).
26. Barash, S., Bracewell, R. M., Fogassi, L., Gnadt, J. W. & Andersen, R. A. Saccade-related activity in the lateral intraparietal area. I. Temporal properties; comparison with area 7a. *J. Neurophysiol.* **66**, 1095 (1991).
27. Barash, S., Bracewell, R. M., Fogassi, L., Gnadt, J. W. & Andersen, R. A. Saccade-related activity in the lateral intraparietal area. II. Spatial properties. *J. Neurophysiol.* **66**, 1109 (1991).
28. Mitra, P. & Bokil, H. *Observed Brain Dynamics.* (Oxford University Press, New York, 2008).
29. Torrence, C. & Compo, G. P. A practical guide to wavelet analysis. *Bull. Amer. Meteor.* **79**, 61–78 (1998).

Acknowledgments

Author contributions

Y.L. and M.C. designed the experiments. M.C., L.W. and Y.L. conducted the experiments. Y.L. and M.C. analyzed the data and prepared all figures. M.C. and Y.L. wrote the manuscript.

Additional information

Supplementary information accompanies this paper at http://www.nature.com/scientificreports